

880nm surface emitting Microcavity Light Emitting Diode

D. Ochoa^a, R. P. Stanley^a, R. Houdré^a, M. Ilegems^a, C. Hanke^b, B. Borchert^b

^aInstitut de Micro et Optoélectronique, Ecole Polytechnique Fédérale de Lausanne,
1015 Lausanne, Switzerland

^bInfineon Technologies CPR PH, Otto-Hahn-Ring 6,
D-81730 Munich, Germany

ABSTRACT

Microcavity light emitting diodes (MCLEDs) are planar emitting devices that can achieve large brightness increase compare to conventional LEDs. We designed and fabricated a GaAs/Al_xGa_{1-x}As surface-emitting MCLED emitting at 880nm. Two InGaAs quantum wells are included in a λ -Al_{0.3}Ga_{0.7}As cavity between two Al_{0.1}Ga_{0.9}As/Al_{0.8}Ga_{0.2}As Bragg mirrors. The top *n*-doped Bragg mirror has 4 pairs, the bottom one is *p*-doped like the substrate and has 20 pairs. The detuning between the source emission wavelength and the Fabry Péroet wavelength is -20nm. It is optimum for an extraction into air. By inserting the bonded MCLED device into an integration sphere we measured a maximum external quantum efficiency of 14% at 10 mA. An epoxy lens is placed on top of the device and the external quantum efficiency is increased up to 20.5% at 10 mA. These values are in good agreement with theoretical calculations if the internal quantum efficiency of the structure is equal to 85%. Additional calculations and measurements are performed and lead to a good physical understanding of the MCLED.

Keywords: Microcavity Light Emitting Diode, External quantum efficiency, Brightness, Fabry-Péroet

1. INTRODUCTION

Microcavity Light Emitting Diodes (MCLEDs) have been of increasing interest for their improved performance over conventional LED's.¹⁻⁹ In a MCLED, the optically active region is placed at an antinode position inside a Fabry-Péroet thin cavity, which size is close to the wavelength of the emitted light. One of the few resonant modes of the Fabry-Péroet is resonant in a direction which is almost normal to the surface of the device. The spontaneous emission going into this mode is mainly extracted because it fits into the escape cone of the semiconductor medium. As a result, the surface extraction efficiency of the MCLED is improved, compared to a conventional LED, as well as its brightness, its directionality, and the spectral linewidth of its emission. MCLEDs are therefore interesting for applications in optical telecommunications, where they perform better than LEDs and have some advantages compared to laser diodes: higher reliability, lower temperature sensitivity, easier fabrication process and no threshold behavior. The present external quantum efficiency record for a GaAs/Al_xGa_{1-x}As is 22% for a substrate emitting MCLED.¹⁰

In the present work, we investigate a GaAs/Al_xGa_{1-x}As MCLED emitting at 880nm by the surface (as opposed to the substrate). The optical design of the MCLED is explained in section 2. Fabrication process and external quantum efficiency measurements are described in section 3. These measurements are analyzed and compared to theoretical calculations in section 4.

2. OPTICAL DESIGN OF THE MCLED STRUCTURE

The refractive index profile of the GaAs/Al_xGa_{1-x}As MCLED heterostructure is shown in figure 1. The Distributed Bragg Mirrors (DBRs) are made of Al_{0.1}Ga_{0.9}As/Al_{0.8}Ga_{0.2}As pairs: 20 pairs for the back mirror and N_1 pairs for the front mirror (to be optimized). Two In_{0.06}Ga_{0.94}As quantum wells (QWs) emitting at 880nm are placed in the middle of an Al_{0.3}Ga_{0.7}As λ -cavity, the Al_{0.3}Ga_{0.7}As material giving a better electronic confinement in the QWs than the GaAs. The GaAs substrate is *p*-doped, as well as the back DBR, the cavity is undoped and the front DBR is *n*-doped. For a better electronic lateral diffusion, a thick (2 μ m) *n*-doped Al_{0.2}Ga_{0.8}As layer is placed between the surface and the front DBR. It provides homogeneous injection conditions for a large range of current densities, and reduces the top *n*-contact shadowing.

Send correspondence to D.O., E-mail: ochoa@dpmail.epfl.ch

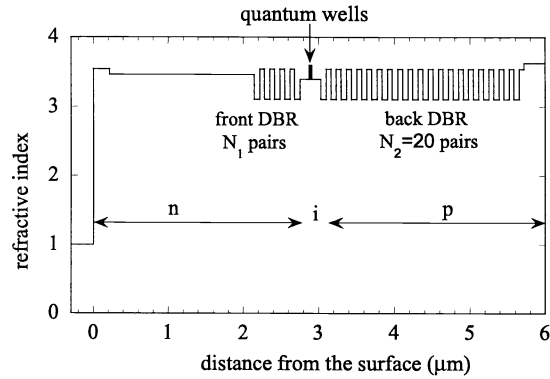


Figure 1. Refractive index profile of the MCLED's heterostructure.

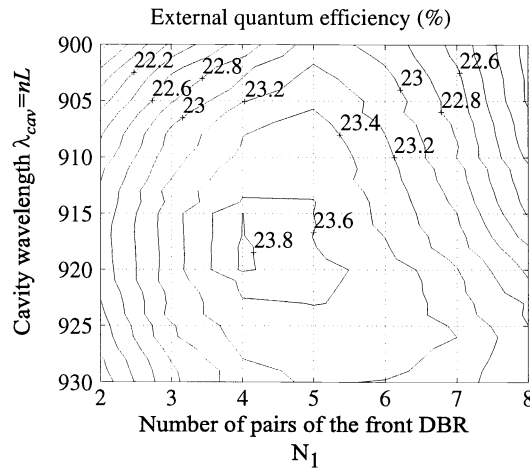


Figure 2. Calculated external quantum efficiency of the MCLED, vs the number of pairs N_1 of the front Bragg mirror and the detuning δ between the source emission wavelength and the Fabry-Pérot wavelength of the microcavity. The calculation is performed for a monochromatic source emitting at 880nm, and for an extraction into epoxy.

The optical design of the MCLED uses the spontaneous emission vertical model described in ref.¹¹ which is based on a plane wave expansion of dipolar emission, and on a transfer matrix method.¹² This model allows a precise calculation of internal and external emission angular dependences. The surface extraction efficiency is obtained by integrating the external power emission on the half-space solid angles. It is maximized by playing with two parameters: the number of pairs of the front DBR (N_1), and the thickness of the λ -cavity (L). The calculation assumptions are the following:

- The internal quantum efficiency is unity: $\eta_{int} = 1$.
- Light recycling into the QWs is not taken into account.
- The external medium has a refractive index of 1.5, like epoxy.
- The DBRs are phase matched with the cavity: $\lambda_{DBR} = \lambda_{cav} = Ln$, where λ_{DBR} is the central wavelength of the DBR and $n=3.4$ (at 880nm), is the refractive index of the cavity medium. λ_{cav} is called the “cavity wavelength”.
- $\text{Al}_x\text{Ga}_{1-x}\text{As}$ refractive indexes are taken from ref.¹³
- The absorption into the QWs is fixed at 0.3% per QW and per pass (3000cm^{-1} for 10nm thick QWs). This value has been obtained by a $\mathbf{k}\cdot\mathbf{p}$ calculation [Siemens, private communication] for a current density of $3\text{A}/\text{cm}^2$, corresponding to a current intensity of 10mA for a $400\mu\text{m}\times 400\mu\text{m}$ square device.

- The free carrier absorption due to doping is set to $\alpha_{dop} = 10\text{cm}^{-1}$ for all the layers.^{14,15}

The optimization of the MCLED is done by maximizing the external quantum efficiency η_{ext} for different values of λ_{cav} and N_1 . The result is shown on figure 2. The optimum is found for $\lambda_{cav} = 920\text{nm}$ ($L = 271\text{nm}$) and $N_1 = 4$ pairs. Then, the maximum monochromatic external quantum efficiency is equal to 23.9%.

3. FABRICATION, EXTERNAL QUANTUM EFFICIENCY MEASUREMENTS

The MCLED device is fabricated with a three steps processing. Small circular n -contacts (Ni Ge Au Ni Au) are first deposited on the n -doped surface. The structure is then wet-etched, forming large circular mesas centered on the n -contact and going deep through the structure, beyond the back DBR. The final processing step is a Ti-Pt-Au metalization of the p -doped surface (substrate) at the feet of the mesas. A schematic section of the device is shown on figure 3 (a).

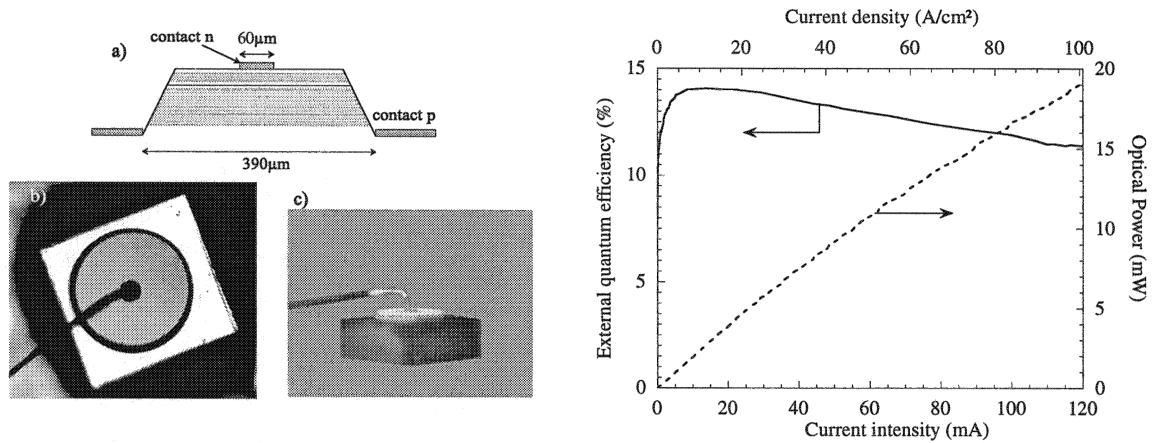


Figure 3. Left part: a) Schematic section of the MCLED device. b) MCLED device cleaved and contacted by wire-bonding. c) Same device under electrical injection. Right part: total external quantum efficiency of the MCLED, placed into an integration sphere. The current is pulsed with a duty cycle of 10%.

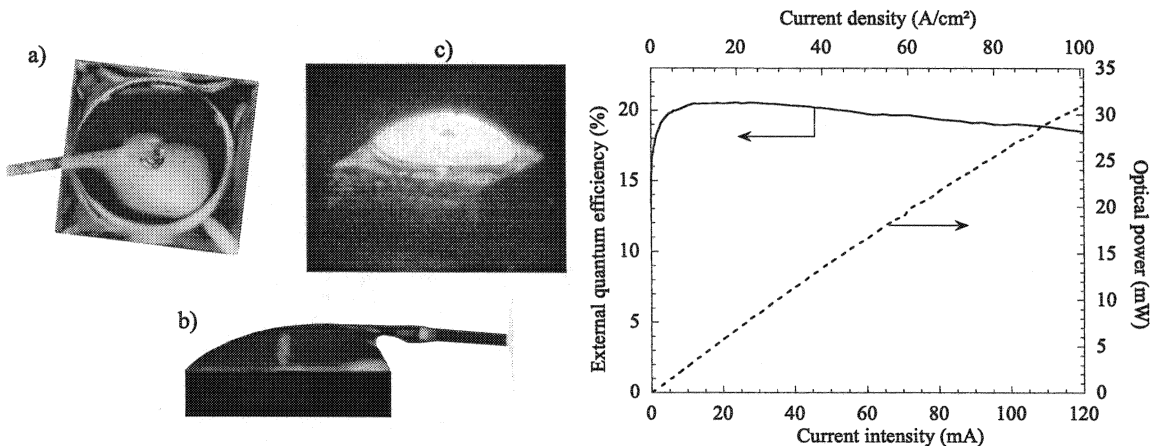


Figure 4. Left part: MCLED device encapsulated into an epoxy lens. a) Top view. b) Side view. c) Under electrical injection. Right part: Total external quantum efficiency of the MCLED encapsulated into an epoxy lens.

The wafer is cleaved into $500\mu\text{m} \times 500\mu\text{m}$ square pieces containing a MCLED each. These pieces are stuck on a TO header with some conducting epoxy, acting as a p -contact with the substrate. The top n -contact is wire-bonded,

as shown on figure 3 (b). The diameter of the bond is $80\mu\text{m}$ and the top diameter of the mesa about $370\mu\text{m}$. The contact shadowing is therefore only $(80/370)^2 = 4.7\%$.

The TO header is inserted into a calibrated integration sphere, measuring the total optical power emitted by the MCLED. The external quantum efficiency is obtained by dividing the optical power by the current intensity and by the photon energy (1.5eV). The result is shown on the figure 3, for a pulsed injection current with a duty cycle of 10%. The quantum external efficiency reaches the maximum value of 14% for a current injection of about 10mA.

The final fabrication step is to encapsulate the device into an epoxy dome. Instead of the usual spherical dome, we used a lens-type shape, as shown on figure 4. The external quantum efficiency measured with the integration sphere is shown on the same figure. Its maximum is 20.6% for a current of 10mA. Figure 5 shows the angular emission pattern of the MCLED with and without the epoxy lens. The directionality of the emission is slightly better with the epoxy lens than without.

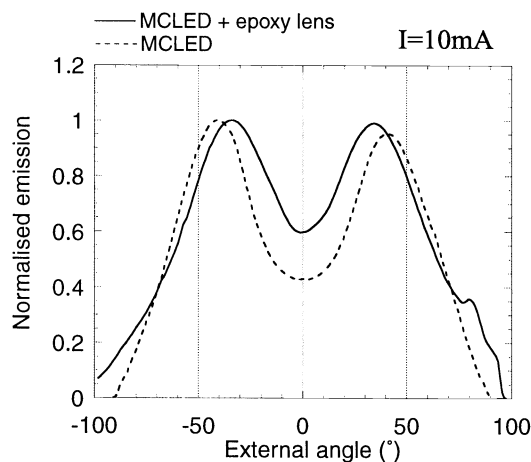


Figure 5. Angular emission pattern of the MCLED without (dashed line) and with an epoxy lens (plain line).

4. ANALYSIS OF THE MCLED MEASUREMENTS

4.1. Reflectivity spectrum

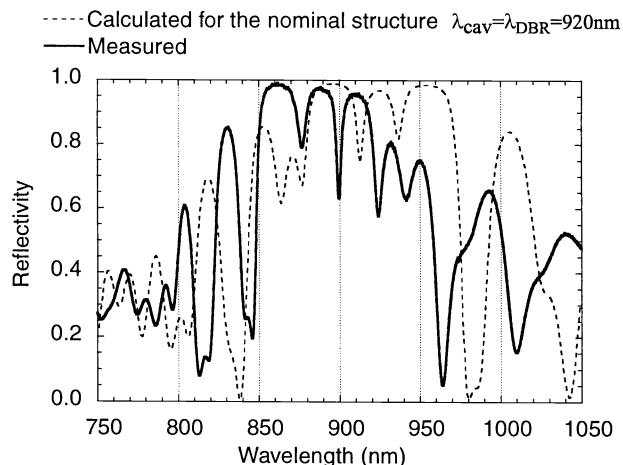


Figure 6. Reflectivity spectra: measured (plain line) and calculated for the nominal structure (dashed line).

The reflectivity spectrum of the MCLED is calculated at normal incidence, using the nominal structure (given by the design of section 2, $\lambda_{cav} = \lambda_{DBR} = 920\text{nm}$) and a transfer matrix model. As shown on figure 6, this spectrum

is different from the measured one. However, the reflectivity spectrum is very sensitive to the thickness of the different layers. It is therefore possible to adjust precisely the heterostructure layer thicknesses, so that its calculated reflectivity spectrum matches the measured one. For this fitting procedure, we play with three parameters:

- The thickness L_d of the thick top electronic diffusion layer (nominal value $L_d = 1920\text{nm}$).
- The “cavity wavelength” $\lambda_{cav} = nL = 3.4L$, where L is the cavity thickness (nominal value: $\lambda_{cav} = 920\text{nm}$).
- The Bragg central wavelength λ_{DBR} (nominal value $\lambda_{DBR} = \lambda_{cav} = 920\text{nm}$).

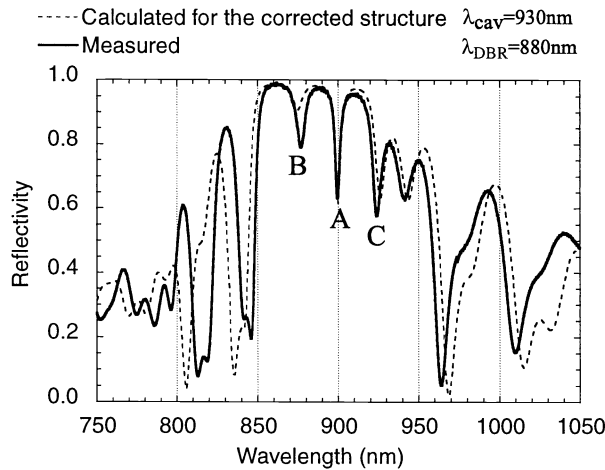


Figure 7. Reflectivity spectra: measured (plain line) and calculated for the corrected structure (dashed line).

λ_{DBR} is changed to adjust the position of the Bragg stopband. Then, L_d and λ_{cav} are modified to fit the position of the resonant modes inside the stopband. The convergence of this procedure is fast and gives the following “fitted” values: $L_d = 1930\text{nm}$, $\lambda_{DBR} = 890\text{nm}$ and $\lambda_{cav} = 930\text{nm}$. The reflectivity spectrum of the corrected structure is calculated using these fitted values and compared with the measured reflectivity spectrum on figure 7. The agreement is good, except for some small refractive index dispersion mismatch, that gives an exaggerated broadening of the overall spectrum. The resonant mode indexed “A” is the cavity mode, the modes “B” and “C” are resonant in the thick electronic diffusion layer (this can be checked by looking at the mode profiles into the structure). By comparing the calculated spectra of figures 6 and 7, it appears that the Fabry-Pérot wavelength of the cavity mode has moved from $\lambda_{FP} = 915\text{nm}$ to $\lambda_{FP} = 900\text{nm}$. This displacement is due to the phase mismatch between the cavity ($\lambda_{cav} = 930\text{nm}$) and the DBRs ($\lambda_{DBR} = 890\text{nm}$) in the corrected structure.

The detuning between the source emission wavelength and the Fabry-Pérot wavelength:

$$\delta = \lambda_0 - \lambda_{FP} \quad (1)$$

is a parameter of first importance concerning the extraction efficiency of a MCLED.^{16,17} For the nominal structure: $\delta = 880 - 915 = -35\text{nm}$, for the corrected one: $\delta = 880 - 900 = -20\text{nm}$. While the nominal structure was optimized for an extraction into epoxy, the corrected structure is optimal for an extraction into air.¹⁸ The angle corresponding to the maximum of external emission into air is close to the ideal value of 45° ¹⁶ (see figure 5).

The detailed thickness and composition values of the corrected structure are given in table 1. The differences in layer thicknesses between this structure and the nominal one do not exceed 3%. The doping profile is kept secret for industrial purpose. The corrected structure will be used for all the following calculations on the MCLED.

4.2. External quantum efficiency calculations

The same assumptions are made as in section 2. The vertical spontaneous emission model of ref¹¹ is still used for the surface extraction calculations. The lateral extraction calculations require an extension of this model, as described in ref.¹⁹

Layer designation	Material	x	thickness (nm)	refractive index at $\lambda = 880\text{nm}$
Contact	$\text{Al}_x\text{Ga}_{1-x}\text{As}$	0.1	220	3.53
Current diffusion	$\text{Al}_x\text{Ga}_{1-x}\text{As}$	0.2	1930	3.46
Front DBR (x4)	$\text{Al}_x\text{Ga}_{1-x}\text{As}$	0.8	71.7	3.1
	$\text{Al}_x\text{Ga}_{1-x}\text{As}$	0.1	63	3.53
	$\text{Al}_x\text{Ga}_{1-x}\text{As}$	0.8	71.7	3.1
Cavity	$\text{Al}_x\text{Ga}_{1-x}\text{As}$	0.3	120.4	3.39
Quantum well	$\text{In}_x\text{Ga}_{1-x}\text{As}$	0.06	12	3.62
Barrier	$\text{Al}_x\text{Ga}_{1-x}\text{As}$	0.3	12	3.39
Quantum well	$\text{In}_x\text{Ga}_{1-x}\text{As}$	0.06	12	3.62
Cavity	$\text{Al}_x\text{Ga}_{1-x}\text{As}$	0.3	120.4	3.39
Back DBR (x20)	$\text{Al}_x\text{Ga}_{1-x}\text{As}$	0.8	71.7	3.1
	$\text{Al}_x\text{Ga}_{1-x}\text{As}$	0.1	63	3.53
Buffer	GaAs		200	3.62
Substrate	GaAs			3.62

Table 1. Corrected heterostructure of the MCLED.

4.2.1. Monochromatic surface extraction

The surface external quantum efficiency η_{ext} is first calculated for a monochromatic source emitting at different wavelengths and for an extraction into air and epoxy. The result is shown in figure 8 (plain line). The curves shape is in good agreement with a basic extraction analysis: the cavity mode is well extracted when its internal resonance angle fits into the window $0 \leq \theta_{in} \leq \theta_c$, where θ_c is the critical angle for total internal reflexion between the source medium (corresponding to θ_{in}) and the external medium. In terms of resonance wavelengths (λ), this translates into:

$$\lambda_{FP} \cos \theta_c \leq \lambda \leq \lambda_{FP} \quad (2)$$

giving: $864\text{nm} \leq \lambda \leq 900\text{nm}$ for an extraction into air ($\theta_c = 16.1^\circ$), and $812\text{nm} \leq \lambda \leq 900\text{nm}$ for an extraction into epoxy ($\theta_c = 25.5^\circ$), in good agreement with the curves of figure 8.

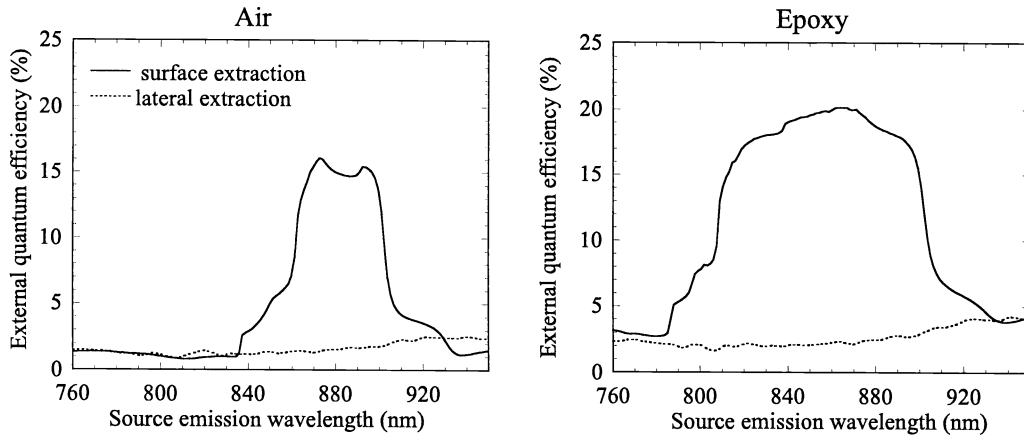


Figure 8. Calculated external quantum efficiency into air and epoxy for a monochromatic source, vs emission wavelength. Surface extraction (plain line) and lateral extraction (dashed line).

4.2.2. Monochromatic lateral extraction

There is only one guided mode propagating in the thin microcavity waveguide. Its typical power decay length is about $80\mu\text{m}$ (TE polarization).^{19,18} Its transmission through a vertical mesa edge is calculated by writing the reflected light in terms of guided and non-guided propagating modes and by applying the field continuity conditions at the interface.^{20,21} This transmission is equal to 63% into air and 80% into epoxy,¹⁸ very close to the usual

Fresnel transmission coefficients. The lateral extraction coefficient of the guided mode is then obtained by a simple ray tracing approach: light rays are considered, having the power decay length and the transmission coefficient of the guided mode, and emitted at various source points and with various propagation directions in the plane of the MCLED. The total transmission of the light ray is then calculated, taking into account multiple reflexions on the side of the circular device, and finally averaged on the emission source point (which is randomly located inside the circle defining the MCLED's mesa, for an homogeneous injection) and on the propagation direction.^{19,18} The resulting extraction coefficient is $\chi_m = 23\%$ into air and $\chi_m = 33\%$ into epoxy (TE). The fraction of power going into the guided mode is $\eta_m = 19\%$ (TE). The lateral external quantum efficiency is then $\eta_{lat} = \eta_m \chi_m$, taking into account TE and TM polarizations. It is shown on figure 8 (dashed line), for an extraction into air and epoxy, and for various emission wavelengths.

4.2.3. Finite linewidth of the source emission

Surface and lateral quantum extraction efficiencies η_{ext} and η_{lat} (shown on figure 8) are averaged on the QWs emission spectrum. This source spectrum is obtained by imaging the lateral emission of the MCLED into an optical fiber (see figure 9). Its deformation due to guided light reabsorption into the QWs is not too large. In the opposite case, the deformation would be larger at 10mA than at 100mA (because the QWs are more absorbent at lower injection) and since the two measured spectra of figure 9 have similar linewidths, the QW emission at 10mA should be larger than at 100mA, which is not realist. To explain the small reabsorption effect, lateral emitted light should mainly come from a region close to the edge of the mesa. This is in agreement with the observed good homogeneity of emission.

The spectrally averaged surface and lateral external quantum efficiencies are finally:

$$\begin{aligned} \text{Air:} \quad & \eta_{ext,poly} = 13.6\% \quad \eta_{lat,poly} = 1.5\% \\ \text{Epoxy:} \quad & \eta_{ext,poly} = 19.2\% \quad \eta_{lat,poly} = 2.4\% \end{aligned} \quad (3)$$

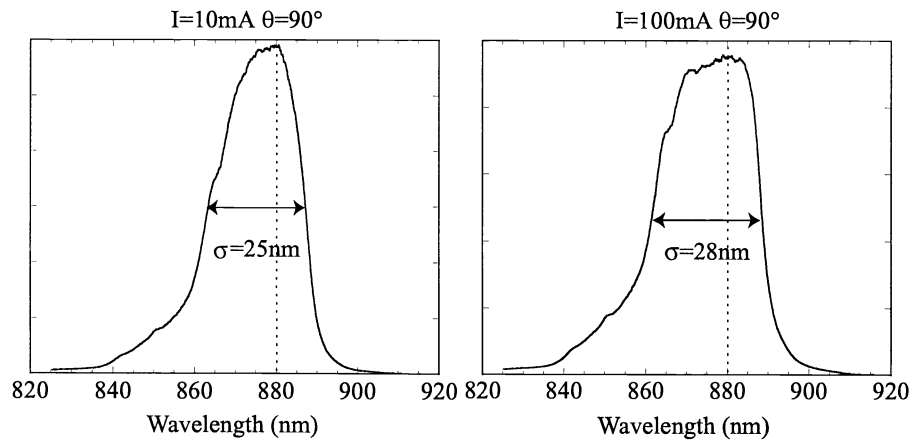


Figure 9. Lateral emission spectrum of the MCLED for current injections of 10mA and 100mA.

4.2.4. Recycling, internal quantum efficiency

The fraction of emitted light that is re-absorbed in the QWs is equal to $\eta_{abs} = 15.3\%$ for an extraction into air and 13.8% for an extraction into epoxy.^{19,18} Due to a multiple absorption-reemission process, the total extraction efficiency is increased by the “recycling factor”:

$$f_{recy} = \sum_{i=0}^{\infty} (\eta_{abs})^i = \frac{1}{1 - \eta_{abs}} \quad (4)$$

All the efficiencies calculated previously were obtained for an internal quantum efficiency of $\eta_{int} = 100\%$. If we now take into account a more realist $\eta_{int} < 1$ and the top contact shadowing ($\tau_{shadow} = 4.7\%$), the total external quantum efficiency (lateral+surface) can be written:

$$\eta_{tot} \simeq \frac{\eta_{int} (\eta_{ext,poly} (1 - \tau_{ombr}) + \eta_{lat,poly})}{1 - \eta_{int} \eta_{abs}} \quad (5)$$

where $\eta_{ext,poly}$ and $\eta_{lat,poly}$ are given by (3), $\eta_{abs} = 15.3\%$ and where the approximation is to neglect the spontaneous emission lifetime modification (Purcell factor) of the QWs in the microcavity. This lifetime modification is small for a planar confinement, as in a MCLED, and do not exceed 10%.¹⁸

The internal quantum efficiency is finally found by matching the total external quantum efficiency given by (5) with the measured values of 14% into air and 20.6% into epoxy (see section 3). For $\eta_{int} = 85\%$ one finds $\eta_{tot} = 14.2\%$ into air and 20% into epoxy.

4.2.5. Extraction from the epoxy lens

It could seem surprising that the agreement between the calculated extraction efficiency into epoxy and the measurement is so good, since the epoxy lens has not the usual spherical dome shape.²² Because of this lens shape, one would expect a fraction of emitted light to be reflected at the interface epoxy/air.

The reason for this good experimental extraction is illustrated in figure 10 (a). A light ray which is reflected at the epoxy/air interface impinges on the MCLED surface with an angle θ_{ext} . It goes into the device with an internal angle $\theta_{in} = \arcsin(1.5/3.5 * \sin \theta_{ext})$, which is necessarily lower than the critical angle $\theta_c = \arcsin(1.5/3.5) \simeq 24^\circ$. However, the reflectivity of the 20 pairs back DBR of the MCLED is high for $0 \leq \theta_{in} \leq 21^\circ$ (stopband). Thus, except for light rays propagating at grazing angles into the epoxy, and at an angle θ_{in} close to θ_c inside the MCLED structure, the back DBR mirror is highly reflective and the light ray goes back into the epoxy with the same angle θ_{ext} .

The overall effect of the lens is to act as a taper (see figure 10 (b)), where multiple reflexions decrease the zenithal angle of the propagating light ray, that finally gets the right incidence on the epoxy/air interface to be extracted.

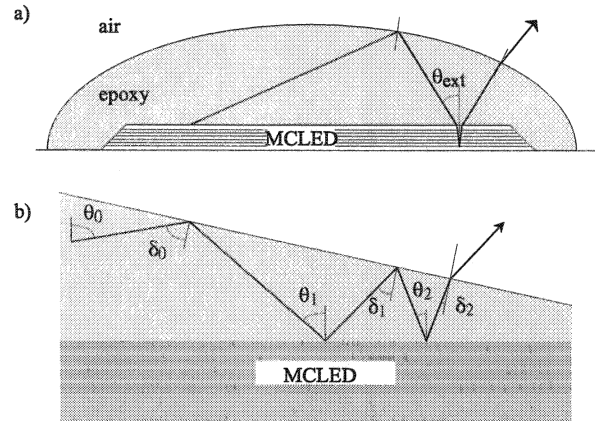


Figure 10. a) Schematic trajectory followed by a light ray inside the epoxy lens, before its extraction into air. b) The epoxy lens acts as a taper, redirecting the light rays towards the normal of the surface, and finally allowing extraction.

4.3. Angularly resolved spectra

In the last part of this article, we analyse the spectral emission of the MCLED at different angles. This will give a good intuitive understanding of the MCLED's extraction mechanism.

The emission spectra are measured at 200 different zenithal angles θ_{ext} and put together in a 3D representation $S_{meas}(\theta_{ext}, \lambda)$ shown in figure 11 (a). This measured 3D representation is in good agreement with the calculated one $S(\theta_{ext}, \lambda)$, shown in figure 11 (b).

In order to calculate $S(\theta_{ext}, \lambda)$, the first step is to evaluate $S_{white}(\theta_{ext}, \lambda)$, the emission spectra corresponding to a white source, i.e. a source emitting the same light power at all wavelengths. $S_{white}(\theta_{ext}, \lambda)$ is shown in figure 11 (c). The three resonant modes of the figure 7 can be easily identified: "A" being the cavity mode, "B" and "C" being resonant in the thick electronic diffusion layer. All these modes follow the "resonance law" in the plane (θ_{ext}, λ) :

$$\lambda = \lambda_{FP} \cos \theta_{in} = \lambda_{FP} \sqrt{1 - \frac{1}{3.4^2} \sin^2 \theta_{ext}} \quad (6)$$

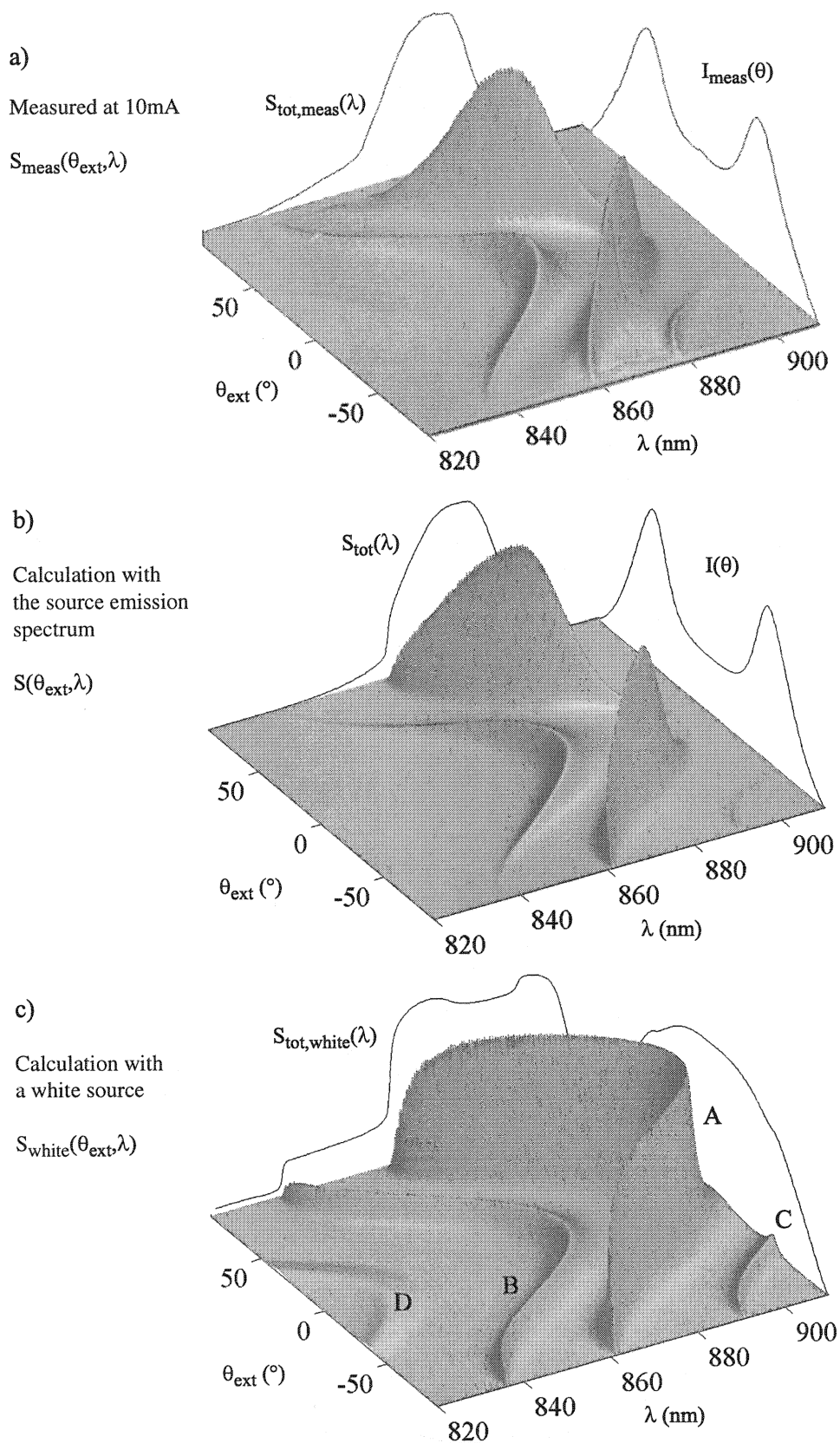


Figure 11. Spectrally and angularly resolved 3D representation of the MCLED's emission. a) Measured for a current injection of 10mA. b) Calculated using the quantum wells emission spectrum. c) Calculated using a white light source, emitting the same light intensity at all wavelengths.

where θ_{in} is the internal angle (corresponding to θ_{ext}) for a propagation in the medium of the microcavity, which refractive index is 3.4. One can check for example, that for the cavity mode ($\lambda_{FP} = 900\text{nm}$) and at grazing incidence ($\theta_{ext} = 90^\circ$), the resonance occurs at $\lambda = 860\text{nm}$, in very good agreement with the figure 11 (c).

As a second step, the spectra $S(\theta_{ext}, \lambda)$ are obtained by multiplying $S_{white}(\theta_{ext}, \lambda)$ with the source emission spectrum, shown in figure 9*. The overall agreement between the calculation $S(\theta_{ext}, \lambda)$ and the measurement $S_{meas}(\theta_{ext}, \lambda)$ is good. However, some differences are noticeable (see for example the mode ‘‘C’’). They are due to some inhomogeneity of the layer thicknesses across the wafer, and to the fact that the measured MCLED was not located exactly where the reflectivity spectrum measurement used to obtain the ‘‘corrected structure’’ was made.

The curves represented in the vertical plane ($\theta_{ext} = 90^\circ$) of the figure 11 correspond to the integral of the various spectra on the solid angles between $-\pi/2$ and $\pi/2$:

$$S_{tot}(\lambda) = \int_{-\pi/2}^{\pi/2} S(\theta_{ext}, \lambda) 2\pi \sin \theta_{ext} d\theta_{ext} \quad (7)$$

idem for $S_{tot,meas}(\lambda)$ and $S_{tot,white}(\lambda)$. $S_{tot,meas}(\lambda)$ corresponds to the ‘‘integrated spectrum’’ that one would measure by placing the MCLED into an integration sphere. $S_{tot}(\lambda)$ is in good agreement with $S_{tot,meas}(\lambda)$. $S_{tot,white}(\lambda)$ corresponds roughly to the monochromatic external quantum efficiency of figure 8. The difference between both curves is equal to the lifetime modification due to the optical confinement. As we said, this modification is small for a purely planar confinement. We checked that it does not exceed 10% in our case.

The curves represented in the vertical plane ($\lambda = 910\text{nm}$) of the figure 11 correspond to the integrated angular diagrams:

$$I(\theta_{ext}) = \int S(\theta_{ext}, \lambda) d\lambda \quad (8)$$

idem for $I_{meas}(\theta_{ext})$. $I_{meas}(\theta_{ext})$ is exactly what would be measured with a Si detector placed in rotation around the sample (see figure 5). The 3D representation allows a better visual understanding of this angular diagram:

- Since the ‘‘ridge’’ of the cavity mode in the 3D plot is almost constant for a white source emission (figure 11 (c)), the maximum of the angular diagram’s lobe is only given by the spectral maximum of the QWs source spectrum. The spectral broadening due to the current injection does not affect the angular position of this lobe.
- The height of the angular diagram at normal incidence ($\theta_{ext} = 0$) depends only on the long-wavelengths side of the source emission spectrum. It intuitively corresponds to the ‘‘cut’’ of the source spectrum into the cavity mode ridge between 880nm and 900nm.

5. CONCLUSION

A GaAs/Al_xGa_{1-x}As 880nm surface emitting MCLED has been optimized, fabricated and characterized. The external quantum efficiency reaches 14% into air and 20.6% with an encapsulation into an epoxy lens for a current of 10mA. The emitted optical power reaches 25mW for a current injection of 100mA (pulsed). These measurements are in good agreement with the theory, if the internal quantum efficiency of the device is equal to 85%. The epoxy lens seems to be as efficient as the usual epoxy spherical dome. An explanation of this effect can be attributed to the 20 pairs back DBR of the MCLED, acting as a very reflective mirror for almost all light rays. Associated with the taper-like shape of the epoxy lens, this back mirror allows multiple reflexions of the light propagating into the epoxy, with a progressive redirection towards normal incidence at the interface epoxy/air.

Spectral measurements were performed at a large number of angles and put together in 3D representations. These representations contain almost all the useful optical information concerning the cavity mode extraction of the MCLED. They allow a good visual understanding of the angular diagram and the integrated spectrum formation.

ACKNOWLEDGMENTS

This work was supported by the European Commission within the framework of the ESPRIT SMILED program.

*Actually, a semi-Gaussian approximation of this source spectrum is used.

REFERENCES

1. H. Yokoyama, K. Nishi, T. Anan, H. Yamada, S. D. Brorson, and E. P. Ippen, "Enhanced spontaneous emission from GaAs quantum wells in monolithic microcavities," *Appl. Phys. Lett.* **57**(26), pp. 2814–2816, 1990.
2. H. Yokoyama, "Physics and device applications of optical microcavities," *Science* **256**, pp. 66–70, 1992.
3. G. Björk, S. Machida, Y. Yamamoto, and K. Igeta, "Modification of spontaneous emission rate in planar dielectric microcavity structures," *Phys. Rev. A* **44**, pp. 669–681, 1991.
4. G. Björk, H. Heitmann, and Y. Yamamoto, "Spontaneous-emission coupling factor and mode characteristics of planar dielectric microcavity lasers," *Phys. Rev. A* **47**(5), pp. 4451–4463, 1993.
5. E. F. Schubert, Y. H. Wang, A. Y. Cho, L. W. TU, and G. J. Zydzik, "Resonant cavity light-emitting diode," *Appl. Phys. Lett.* **60**(8), pp. 921–923, 1992.
6. N. E. J. Hunt, E. F. Schubert, D. L. Sivco, A. Y. Cho, and G. J. Zydzik, "Power and efficiency limits in single-mirror light emitting diodes with enhanced intensity," *Electron. Lett.* **28**(23), pp. 2169–2171, 1992.
7. N. E. J. Hunt, E. F. Schubert, R. A. Logan, and G. J. Zydzik, "Enhanced spectral power density and reduced linewidth at $1.3\mu\text{m}$ in an InGaAsP quantum well resonant-cavity light-emitting diode," *Appl. Phys. Lett.* **61**(19), pp. 2287–2289, 1992.
8. E. F. Schubert, N. E. J. Hunt, M. Micovic, R. J. Malik, D. L. Sivco, A. Y. Cho, and G. J. Zydzik, "Highly efficient light-emitting diodes with microcavities," *Science* **265**, pp. 943–945, 1994.
9. N. E. J. Hunt, "High efficiency, narrow spectrum resonant cavity Light Emitting Diodes," in *Confined Electrons and Photons*, E. Burstein and C. Weisbuch, eds., pp. 703–714, Plenum Press, (New York), 1995.
10. H. D. Neve, J. Blondelle, P. V. Daele, P. Demeester, and R. Baets, "Recycling of guided mode light emission in planar microcavity Light Emitting Diodes," *Appl. Phys. Lett.* **70**, pp. 799–801, 1997.
11. R. P. S. H. Benisty and M. Mayer, "Method of source terms for dipole emission modification in modes of arbitrary planar structures," *J. Opt. Soc. Am. A* **15**, pp. 1192–1201, 1998.
12. W. Lukosz, "Light emitted by multipole sources in thin layers. I. Radiation patterns of electric and magnetic dipoles," *J. Opt. Soc. Am.* **71**, pp. 744–754, 1981.
13. S. Adachi, "Optical properties of AlGaAs: Transparent and interband transition regions (tables)," in *Properties of Aluminium Gallium Arsenide*, S. Adachi, ed., vol. 7, pp. 126–140, Inspec Publication, 1991.
14. K. J. Ebeling, ed., *Integrated Opto-electronics*, Springer-Verlag, New York, 1991.
15. C. Dill, *Fabrication and characterization of high efficiency microcavity light emitting diodes*. PhD thesis, Ecole Polytechnique Fédérale de Lausanne, DP IMO EPFL 1015 Lausanne CH, 1999.
16. H. Benisty, H. D. Neve, and C. Weisbuch, "Impact of planar microcavity effects on light extraction : I. basic concepts and analytical trends," *IEEE J. Quantum Electron.* **34**, p. 1612, 1998.
17. D. Ochoa, R. Houdré, R. P. Stanley, U. Oesterle, and M. Ilegems, "Device simultaneous determination of the source and cavity parameters of a microcavity Light-Emitting Diode," *J. Appl. Phys.* **85**, pp. 2994–2996, 1999.
18. D. Ochoa, *Diodes électroluminescentes planaires à haut rendement d'extraction lumineuse*. PhD thesis, Ecole Polytechnique Fédérale de Lausanne, DP, Institut de Micro et Optoélectronique, EPFL, 1015 Lausanne Switzerland, 2000.
19. D. Ochoa, R. Houdré, R. P. Stanley, M. Ilegems, H. Benisty, C. Hanke, and B. Borchert, "Spontaneous emission model of lateral light extraction from heterostructure light-emitting diodes," *Appl. Phys. Lett.* **76**(22), pp. 3179–3181, 2000.
20. T. Ikegami *IEEE J. Quantum Electron.* **8**, p. 470, 1972.
21. H. Kressel and J. K. Butler, eds., *Semiconductor Lasers and Heterojunction LEDs*, Academic Press, New York, 1977.
22. W. N. Carr, "Photometric figures of merit for semiconductor luminescent sources operating in spontaneous mode," *Infrared Physics* **6**, pp. 1–19, 1966.